不連続な風の剪断による閉鎖性水域の吹送流

誌名	水産工学
ISSN	09167617
著者	森, 健 四ヶ所, 四男美 平松, 和昭
巻/号	37巻3号
掲載ページ	p. 195-201
発行年月	2001年2月

Fisheries Engineering
Vol.37 No.3, pp.195～201, 2001

[Research Article]

Wind-Induced Flow in a Closed-Water Area with Discrete Wind Shear

Ken MORI*1, Shiomi SHIKASHO*1 and Kazuaki HIRAMATSU*1

Abstract

In this study, we examine a two-dimesional steady-state wind-induced flow in a closed-water area by use of a numerical simulation method with the k-ε turbulence model. We consider the properties of flow induced by a discrete wind shear stress due to a film of algae that partially covers the water surface. We found that the distributions of mean velocity, turbulent kinetic energy, energy dissipation rate and kinematic eddy viscosity are remarkably affected by the discrete wind shear on the leeward end of the film.

1. Introduction

A flow in closed-water areas (estuaries, reservoirs and lakes) is primarily caused by wind shear, which is a wind-induced flow. The wind-induced flow determines both horizontal and vertical distributions of phytoplankton cells, significantly affecting water quality in the closed-water area. Therefore, it is very important for the water environment dynamics in such an area that both the mean and turbulent characteristics in the wind-induced flow are known. In particular, it is useful to know both the horizontal and vertical distributions of kinematic eddy viscosity, because they are closely related to both turbulent transport and turbulent mixing of environmental materials.

Experimental studies have examined wind-induced flow properties ; however, for the most part they examined the wind-shear-induced mean flow characteristics near the water surface[1), 2)]. Determining turbulent flow characteristics in the wind-induced flow is very important for understanding turbulent transport and turbulent mixing in the water area. In addition, there have been no study of the characteristics of mean and turbulent flows generated by a discrete steady-state wind shear affected by a film on the surface.

In the present study we thus examine the applicability of the k-ε turbulence model[3)] with the object of understanding the wind-induced flow and turbulence in closed-water areas that have relatively shallow depth and are covered partially with film algae on the surface. The k-ε model is able to simultaneously give the distributions of the kinematic eddy viscosity which are the most important turbulence variables, because both mean and turbulent variables are analyzed as unknown in the model.

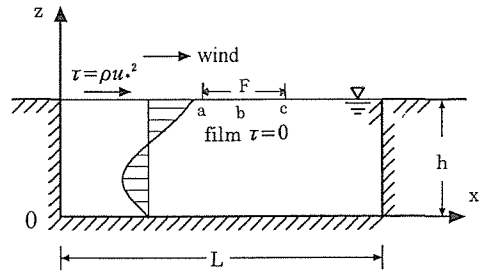

Fig. 1 Definition of Wind-Induced Flow System.

First, the present study uses computations and laboratory experiments to examine the flow without the film on the surface in order to determine whether the k-ε model is appropriate for analyzing the wind-induced flow. Secondly, the study examines the effects of the surface film on the wind-induced flow.

2. Numerical Calculation Method

1) Governing Equations

The present numerical simulations are concerned with a steady-state two-dimensional wind-induced flow in a uniform rectangular channel of constant depth as schematically depicted in **Fig. 1**. L is the water area length in the x direction and h is the water depth.

The continuity equation for an incompressible fluid is

Received May 19, 2000, Accepted October 27, 2000
Key words : Wind-induced flow, Closed-water areas, k-ε turbulence model, Coefficient of kinematic eddy viscosity, Numerical analysis

*1 Department of Bioproduction Environmental Science, Faculty of Agriculture, Kyushu University, Hakozaki 6-10-1, Higashiku, Fukuoka, 812-8581, Japan

$$\frac{\partial u}{\partial x}+\frac{\partial w}{\partial z}=0 \qquad \cdots\cdots(1)$$

in which u and w are the velocities in the x and z directions, respectively.

The x and z components of the momentum equations are

$$u\frac{\partial u}{\partial x}+w\frac{\partial u}{\partial z}=-\frac{1}{\rho}\frac{\partial p}{\partial x}+\frac{\partial}{\partial x}\left(\nu_t\frac{\partial u}{\partial x}\right)+\frac{\partial}{\partial z}\left(\nu_t\frac{\partial u}{\partial z}\right) \qquad \cdots\cdots(2)$$

$$u\frac{\partial w}{\partial x}+w\frac{\partial w}{\partial z}=-g-\frac{1}{\rho}\frac{\partial p}{\partial z}+\frac{\partial}{\partial x}\left(\nu_t\frac{\partial w}{\partial x}\right)+\frac{\partial}{\partial z}\left(\nu_t\frac{\partial w}{\partial z}\right) \qquad \cdots\cdots(3)$$

in which ρ is water density, p is pressure, g is gravity acceleration and ν_t is kinematic eddy viscosity.

A two-equation turbulence model, that is, a standard k-ε turbulence model, includes an expression for the kinematic eddy viscosity ν_t and two coupled differential equations for the turbulent kinetic energy k and the dissipation of this enegy, ε which for two-dimensional flows at high Reynolds numbers are, respectively ;

$$\nu_t=C_\mu\frac{k^2}{\varepsilon} \qquad \cdots\cdots(4)$$

$$u\frac{\partial k}{\partial x}+w\frac{\partial k}{\partial z}=\frac{\partial}{\partial x}\left(\frac{\nu_t}{\sigma_k}\frac{\partial k}{\partial x}\right)+\frac{\partial}{\partial z}\left(\frac{\nu_t}{\sigma_k}\frac{\partial k}{\partial z}\right)+G-\varepsilon \qquad \cdots\cdots(5)$$

$$u\frac{\partial \varepsilon}{\partial x}+w\frac{\partial \varepsilon}{\partial z}=\frac{\partial}{\partial x}\left(\frac{\nu_t}{\sigma_\varepsilon}\frac{\partial \varepsilon}{\partial x}\right)+\frac{\partial}{\partial z}\left(\frac{\nu_t}{\sigma_\varepsilon}\frac{\partial \varepsilon}{\partial z}\right)+C_1\frac{\varepsilon}{k}G-C_2\frac{\varepsilon^2}{k} \qquad \cdots\cdots(6)$$

in which

$$G=\nu_t\left\{2\left[\left(\frac{\partial u}{\partial x}\right)^2+\left(\frac{\partial w}{\partial z}\right)^2\right]+\left(\frac{\partial u}{\partial z}+\frac{\partial w}{\partial x}\right)^2\right\}$$

σ_k is an effective turbulent Prandtl number with a value approximately equal to unity, σ_ε is an effective Schmidt number, C_μ is a numerical constant in turbulent eddy viscosity expression and C_1 and C_2 are numerical constants.

2) Numerical Scheme

In the present numerical simulations, the equations are solved by use of a SIMPLE[4] method with variables defined on a space-staggered rectangular grid scheme. Further, the governing equations are discretized by in a control volume technique. The advection terms are then approximated by upwind differences in space and the diffusion terms and first order space differential terms by central differences in space.

The grid size is rectangular, with spacings of $\Delta x=L/100$ and $\Delta z=h/50$, where Δx and Δz are grid size in the x and z directions. The technique of computations for the near surface , the near bottom and the near side walls uses the wall's rule.

The boundary condition on the water surface is $\tau=\rho u_*^2$ in which τ is the surface shear stress induced by the wind in the x direction, ρ is water density and u_* is the surface shear velocity for the water. At the side walls and the bottom, no slip velocity conditions are used and the vertical velocity component normal to the water surface is taken to be zero. The pressure condition is assumed to be the rigid-lid. The model constants $\sigma_k=1.0$, $\sigma_\varepsilon=1.3$, $C_1=1.44$, $C_2=1.9$ and $C_\mu=0.09$ are used in the calculations.

3. Model Verification

1) Computational Conditions

Laboratory measurements of wind-induced flow are used to check on the ability of the model to reproduce real flows. **Table 1** gives hydraulic conditions used in order to compare computations with laboratory measurements. The flows for the aspect ratios $L_h=L/h=6$ and 17 used are the cavity and the nearly horizontal, respectively. Flow properties are measured with a two-dimensional laser-doppler velocimeter (LDV) (Kanomax Japan Inc.).

Table 1 Hydraulic conditions

case	u_* (cm/s)	h (cm)	L (cm)	L_h
1	0.54	30	180	6
2	2.04	30	500	17

2) Results

Comparisons of computed and measured mean velocity u in the x direction, tubulent kinetic energy k and kinematic eddy viscosity ν_t values normalized by the surface shear velocity u_* and the depth h at the fetch $L/2$ are shown in **Fig. 2.** Kinematic eddy viscosity μ_t were calculated by use of the equation defined by Boussnesq, $-\rho\overline{u'v'}=\mu_t(\partial u/\partial z)$, in which $-\rho\overline{u'v'}$ is the Reynolds stress.

Fig. 2 shows that the computed and measured values for u, k and ν_t are in good agreement except near the surface, where laboratory measurements tend to lack accuracy due to surface wave and turbulence generated by the wind action.

Fig. 2 indicates that the k-ε turbulence model is sufficiently applicable to analyze the wind-induced flow. The figure shows that the near-surface flow generated by wind shear produces much turbulent kinetic energy k due to its great velocity gradient. **Fig. 2** also shows that there is no

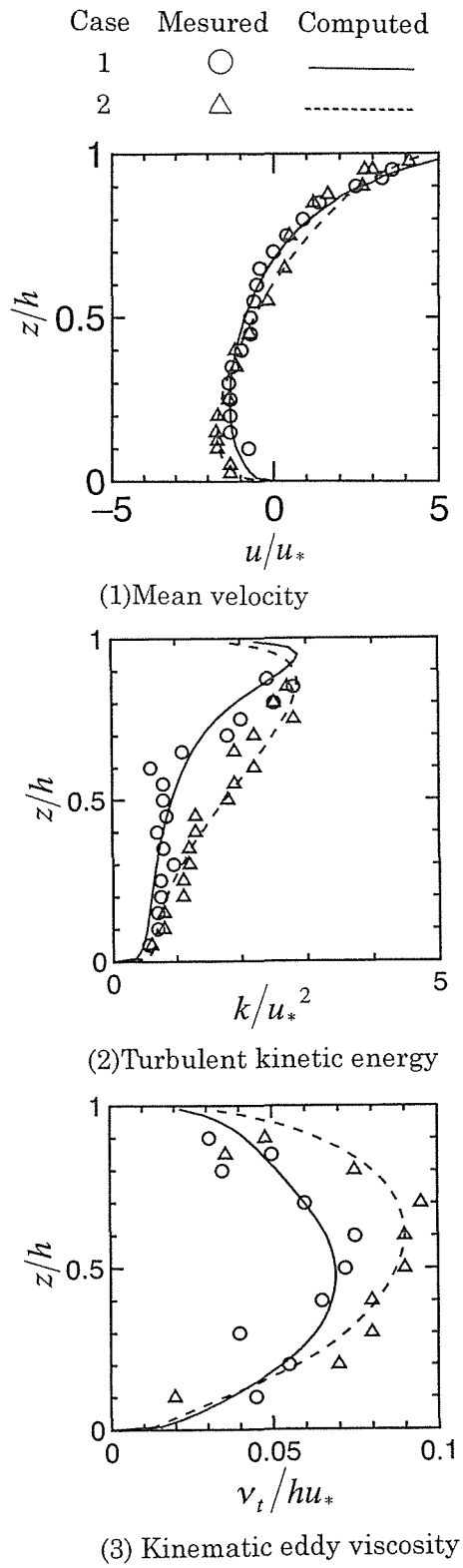

Fig. 2 Comparison of Computed and Measured Distributions for Wind-Induced Flow at the Fetch $L/2$.

Table 2 Computational case

Run	u_* (cm/s)	h (m)	L (m)	L_h	λ (%)
1	0.54	5.0	100.0	20.0	0
2	0.54	5.0	100.0	20.0	5
3	0.54	5.0	100.0	20.0	9
4	0.54	5.0	100.0	20.0	17

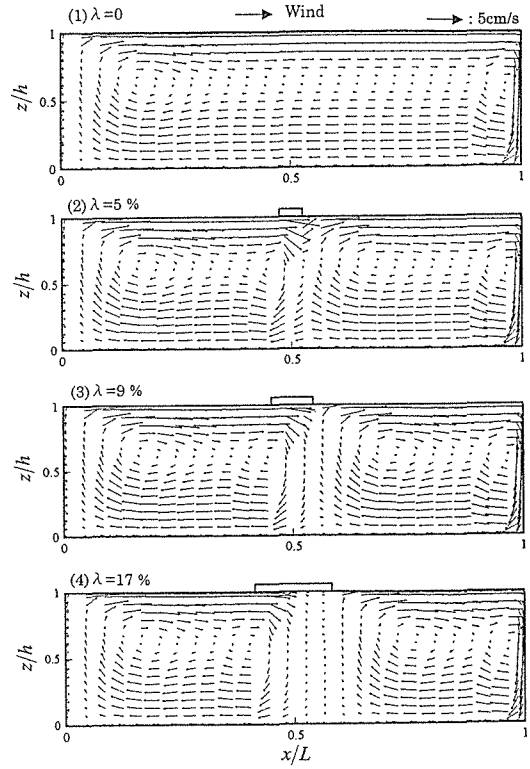

Fig. 3 Flow Patterns for Various Values of λ.

difference in the point of shift depth from drift current to return current in the computed and measured velocity distributions. Comparisons of the computed velocities and measured velocities show that the present model is sufficient to accurately predict k and ν_t values.

4. Model Application to Wind-Induced Flow with Surface Film

1) Computational Conditions

The computations for model application are conducted for the aspect ratio L_h=20 (h=5m, L=100m), because the wind-induced flow is nearly horizontal when L_h is over 16 according to the results of preliminary computations conducted for L_h=1～40 and u_*=0.54, 0.90, 1.80cm/s. The computations examine the wind-induced flow in the closed-water area where algae cells partially cover and rest in the

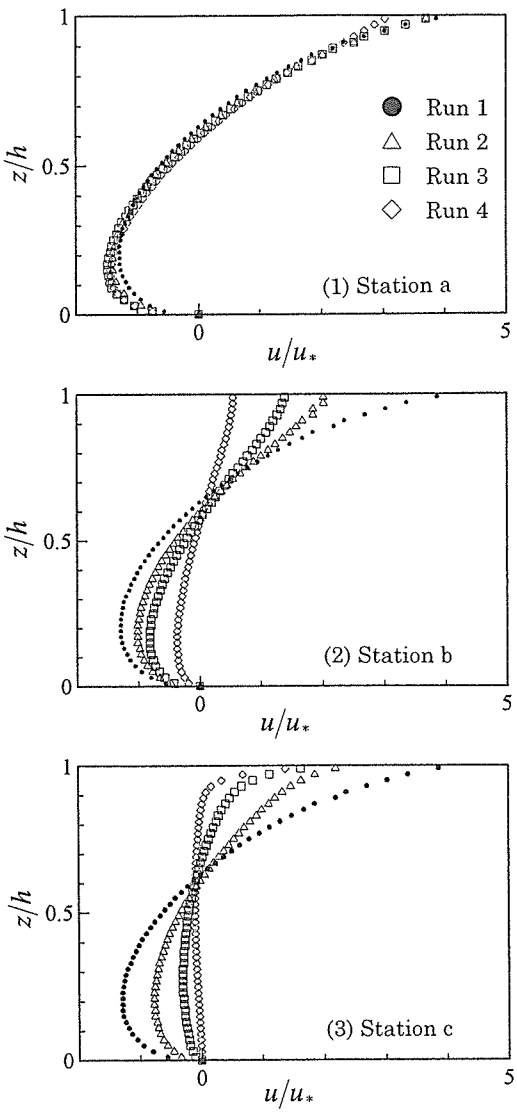

Fig. 4 Computed x-Direction Mean Velocity Distributions for Various Values of λ.

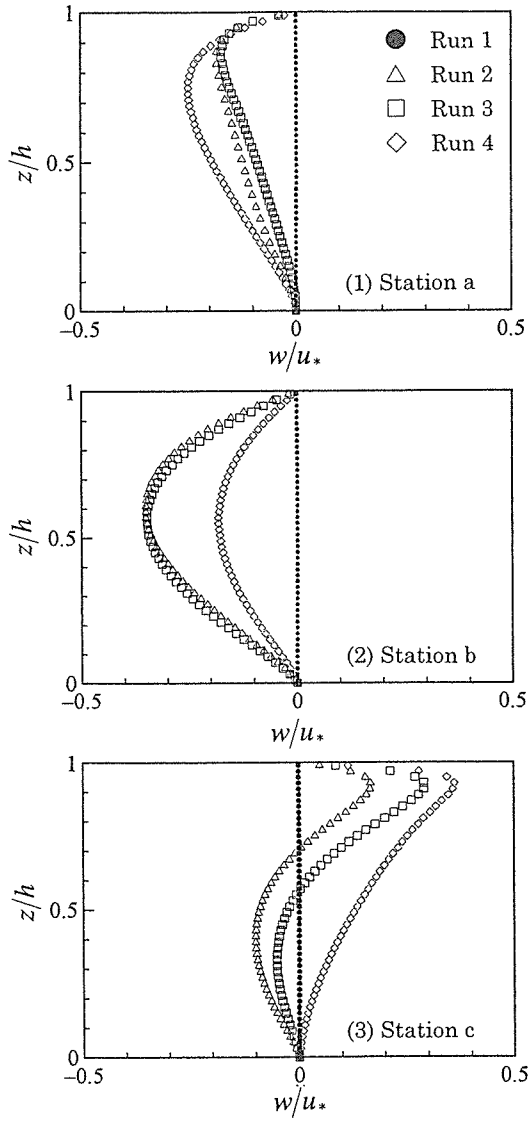

Fig. 5 Computed z-Direction Mean Velocity Distributions for Various Values of λ.

Table 3 Ratios of Γ_λ to $\Gamma_{\lambda=0}$, β

Run	λ (%)	Section b	Section c
2	5	0.75	0.59
3	9	0.57	0.25
4	17	0.24	0.09

center of the water surface. The computations are also conducted for various values of $\lambda = F/L$, which is the ratio of the surface film length F to the water surface length L. The surface film is assumed as a wall in those calculations. **Table 2** gives computational conditions for the model application. The symbols a, b and c in **Fig. 1** represent the windward end, center and leeward end of the surface film, respectively.

2) Results

Fig. 3 shows the computed flow patterns for Run 1 (λ=0), 2 (λ=5%), 3 (λ=9%) and 4 (λ=17%). It is clear from the figure that the discrete wind shear due to the partial film on the surface has a major effect on the wind-induced flow patterns. The computation results indicate that two clockwise circulation patterns clearly appear as the magnitude of λ increases, and the film finally divides the wind-induced flow field into two independent regions.

The computed u, w velocity profiles normalized by the surface shear velocity u_* for various values of λ are depicted in **Figs. 4** and **5**, respectively. **Fig. 4** indicates the effect of λ on the distributions of the horizontal velocity u.

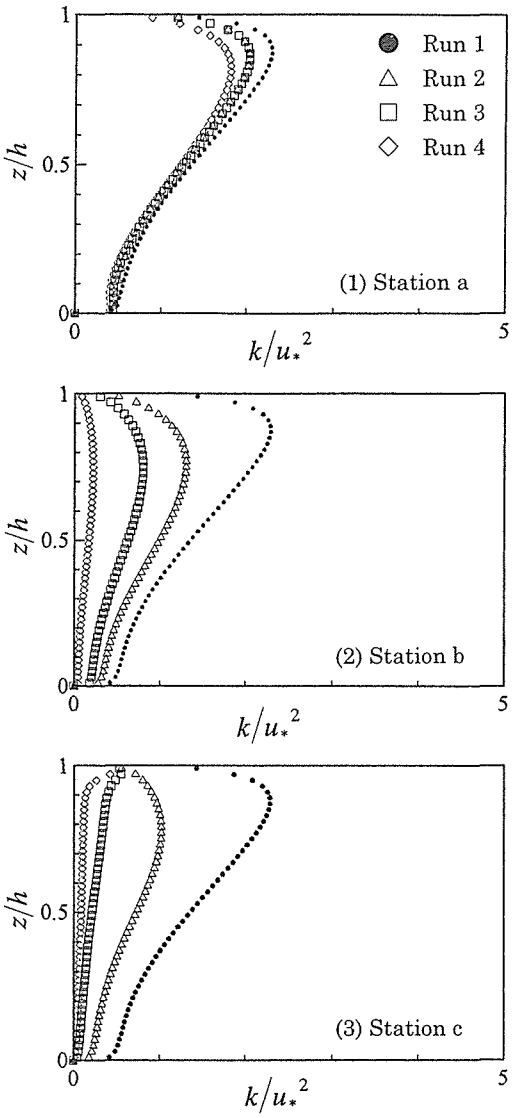

Fig. 6 Computed Kinetic Turbulent Energy Distributions for Various Values of λ.

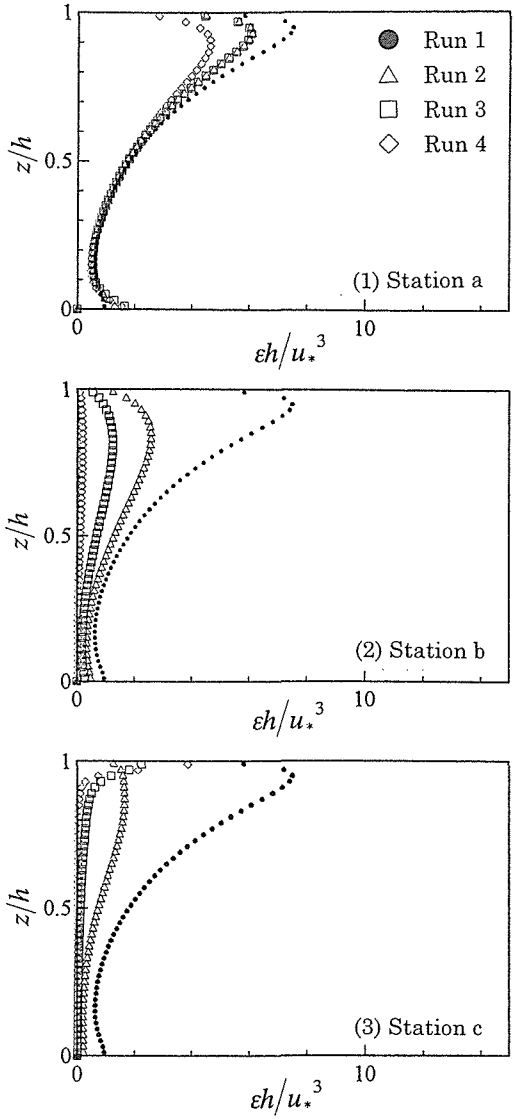

Fig. 7 Computed Energy Dissipation Rate Distributions for Various Values of λ.

Table 3 gives the calculated values of the ratio $\beta=(\Gamma_\lambda/\Gamma_0)$ in which Γ_λ and Γ_0 represent circulation flow rates for $\lambda=\lambda$ and $\lambda=0$, respectively. The circulation flow rate is defined as the expression $\Gamma=\int_0^h u dz$. The influence of λ on Γ_λ is quite significant in the regions right below the film and at the leeward end of the film, although there is no significant influence at the windward end.

Fig. 5 indicates that the computed distributions of vertical velocity w are also influenced by λ. In the case of $\lambda\neq 0$, vertical velocities are generated below the film, although there is no vertical velocity except the side walls for $\lambda=0$. **Fig. 5** also shows that the production of turbulent kineticenergy based on $\partial w/\partial z$ is distinguished below the film.

The computed k and ε profiles in the vertical direction for various values of λ are depicted in **Figs. 6** and **7**, respectively. These diagrams show that both k and ε values are large near the surface and smaller toward the bottom, because the turbulent kinetic energy based on the sheared flow is produced in large quantities near the surface.

As mensioned above (see **Figs. 4** and **5**), **Figs. 6** and **7** indicate that the k and ε profiles are also remarkably influenced by the value of λ. The k profiles for small values of λ increase to the depth of the maximum value of k and then decrease towards the bottom, while the extreme value in the k profiles disappear with increasing λ, because the production of k based on surface sheared flow reduces owing to the influence of the film. Such tendencies are

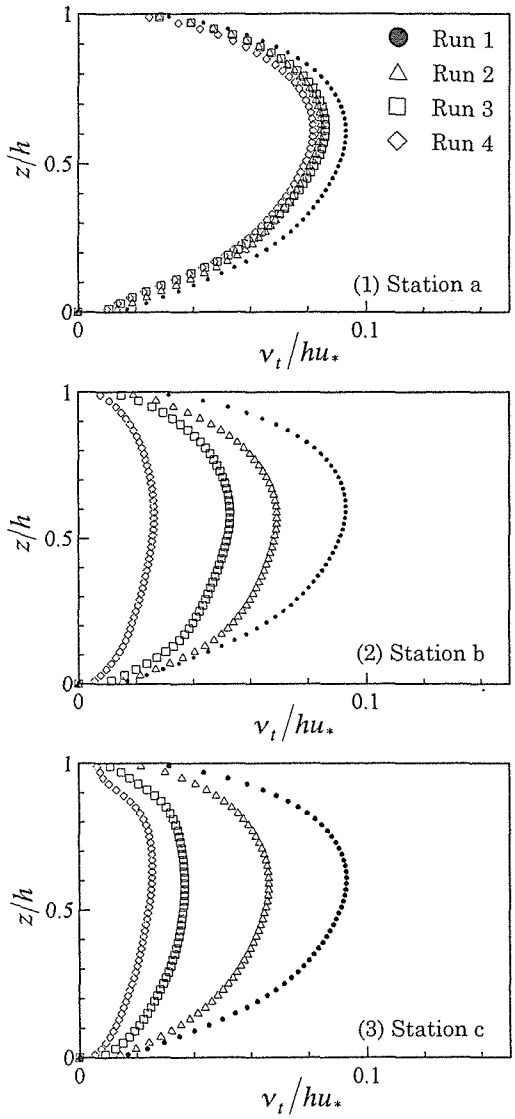

Fig. 8 Computed Kinematic Eddy Viscosity Distributions for Various Values of λ.

remarkable at the leeward end of the film. The computed turbulent eddy viscosity ν_t profiles in vertical for various values of λ are shown in **Fig. 8**. The ν_t distributions are parabolic and are remarkably influenced by the values of λ. Although the maximum value $(\nu_{t,\max})_\lambda$ for various values of λ decrease with incresing λ compared with the maximum value $(\nu_{t,\max})_0=0.09$ for $\lambda=0$, the depth having the maximum values of ν_t is immovable with increasing λ.

Table 4 Ratios of $(\nu_{t,\max})_\lambda$ to $(\nu_{t,\max})_{\lambda=0}$, γ

Run	λ	Section a	Section b	Section c
2	5	1.05	0.74	0.71
3	9	1.04	0.48	0.39
4	17	1.02	0.28	0.27

Table 4 gives the calculated values of ratio $\gamma(=(\nu_{t,\max})_\lambda/(\nu_{t,\max})_0)$ of $(\nu_{t,\max})_\lambda$ for various values of λ to $(\nu_{t,\max})_0$ for $\lambda=0$ in which $(\nu_{t,\max})_\lambda$ is the maximum value of turbulent eddy viscosity for each value of λ. The γ values are influenced by discrete wind shear due to the surface film. The results indicate that a capacity of turbulent transport and turbulent mixing near the surface film decrease greatly with increasing λ.

5. Conclusions

We reached the following conclusions for the model we examined :

(1) The k-ϵ turbulence model can be sufficiently applied to analyze the wind-induced flow.

(2) The discrete wind shear due to the surface film divides the wind-induced flow field into two independent regions.

(3) The mean velocities, turbulent kinetic energy, energy dissipation rate and kinematic eddy viscosity distributions have a major effect on the discrete wind shear at the leeward end of the film.

(4) The turbulent transport and mixing near the film decrease greatly if the film's length is increased.

References

1) J. Wu : Wind-Induced Drift Currents, J. Fluid Mech., Vol. 68, pp. 49-70, 1975.

2) I.K. Tsanis : Simulation of Wind-Induced Water Currents, J. Hydraulics Div., ASCE, Vol. 115, No. 8, pp. 1113-1134, 1989.

3) K. Michioku, G. Tsujimoto and M. Miyamoto : Flow and Mixing Properties in Wind-Induced Density Currents, Annual Journal of Hydraulic Engineering, JSCE, Vol. 37, pp. 293-298, 1993 (in Japanese with English abstract)

4) S.V. Patanker : Numerical Heat Transfer and Fluid Flow. Transl. by Y. Mizutani and M. Katsuki, Hemisphere Pub. Co., U.S.A., 1980 (in Japanese).

不連続な風の剪断による閉鎖性水域の吹送流

森　　健・四ヶ所　四男美・平　松　和　昭

和　文　要　旨

本研究は，閉鎖性水域における鉛直２次元定常流の吹送流特性に関して，標準型 k-ε 乱流モデルを適用した数値解析により検討したものである。

流れ場は，水面の一部が藻類などで薄膜状に覆われ，風の剪断応力が不連続的に作用する状態を想定している。

数値解析の結果から，このような流れ場における吹送流の平均流速，乱流エネルギー，エネルギー散逸率および渦動粘性係数の鉛直分布は，薄膜部の風下端でその影響がとくに大きいことが示された。

2000年５月19日受付，2000年10月27日受理
キーワード：吹送流，閉鎖性水域，k-ε 乱流モデル，渦動粘性係数，数値解析
九州大学大学院農学研究院生産環境科学部門　〒812-8581 福岡市東区箱崎6-10-1